Empirical Eigenanalysis of Indoor UWB Propagation Channels

†Rachid Saadane, ‡Aawatif Menouni, ‡Raymond Knopp, †Driss Aboutajdine
‡Mobile Communications Laboratory Eurecom Institut Sophia Antipolis, France
†GSCM, faculté des sciences Agdal, Rabat, Maroc
e-mail: {saadane,menouni,knopp}@eurecom.fr

***Abstract*— This work aims at characterizing the second order statistics of indoor Ultra-Wideband (UWB) channels using channel sounding techniques. We present measurement results for different scenarios conducted in a laboratory setting at Institut Eurecom. These are based on a eigen-decomposition of the channel autocovariance matrix, which allows for determining the growth in the number of significant degrees of freedom of the channel process as a function of the signaling bandwidth as well as the statistical correlation between different propagation paths. We show empirical eigenvalue distributions as a function of the signal bandwidth for both line-of-sight and non line-of-sight situations. Furthermore, we give examples where paths from different propagation clusters (possibly arising from reflection or diffraction) show strong statistical dependence.**

I. INTRODUCTION

The use of Utra-Wide Band (UWB) signaling techniques are being considered for short-range indoor communications, primarily for next generation high bit-rate *Wireless Personal Area Networks (WPAN)*. Initial work in this direction were carried out by Sholtz [1], [2], using the most common form of signaling based on short-term impulses, where information is carried in their position. Such techniques, as well as others are being considered in the standardization process of the IEEE 802.15.3a WPAN proposal [3]. At the same time, regulatory aspects are quickly being defined by the FCC. The expected bandwidths of these systems are one the order of gigahertz, which has significant implications both for systems design and implementation. The goal of this work is to determine the effects of these extremely large system bandwidths on the second order statistics of the propagation channel. Other studies on the UWB propagation channel have been appearing, for instance [4]-[7]. [4]–[7]. We use state-of-the-art wideband measurement equipment to determine the number of significant degrees of freedom of the propagation channel, or equivalently the number of resolvable multipath components, based on sub-space techniques. This is related to the diversity order or richness of the indoor channel. Measurements are carried out under different propagation scenarios, namely line-of-sight and non-line-of-sight short-range indoor communications. Section II describes the measurement equipment used in this study as well as the propagation environment. In section III we outline the sub-space methods used for analyzing the second order statistics of the propagation channel. Section IV describes the numerical results and section V presents the conclusions of this study.

II. UWB CHANNEL MEASUREMENT

A. Equipment and Measurement Setup

The measurement used in this study is a wideband vector network analyzer (VNA) which allows complex transfer function (e.g. S_{21}) parameter measurements in the frequency range extending from 10 MHz to 20 GHz. This instrument has low inherent noise <-110 dBm (measurement bandwidth 10 Hz) and high measurement speed <0.5 ms/point. With a maximum number of frequency tones equal to 2001 for scanned bandwidth of 2 GHz, the measurement characteristics are as follows: Maximum delay Multipath signals with absolute delays up to T_{max} may be recorded, and the sampling rate corresponds to 1MHz. The antennas employed in this study are omni-directional and are placed in the vertical plane. For each transmitter antenna position, measurement is made by moving the receiving antenna to 50 locations with 1 cm spacing and by setting the frequency range from 3.1 GHz to 10 GHz. The antennas are not perfectly matched across the entire band, with a VSWR (Voltage Standing Wave Ratio) varying from 2 to 5 (for example an efficiency about 82% at 5.2 GHz [8]) as shown in Figure 1. The VNA records the variation (amplitude and phase) of N tones across the frequency range. These complex data are acquired remotely using the RSIB protocol over an Ethernet network and off line signal processing is done in MATLAB. The measurement system is shown in Figure 2. The frequency range corresponds to the start and stop frequencies of the sweep cycle programmed in the VNA. The number of samples is the number of tones of the measured vector with frequency range from 3 to 9 GHz, Frequency center $F_{center} = 6$ GHz, $N_{samples} = 3 * 2001$, giving a frequency resolution $\Delta f = 1$ MHZ. The corresponding time domain resolution is $T = 167$ ps, as which is obtained by concatenated a bands with large 2 GHz for each one, from 2 GHz to 5GHz, 5GHz to 7GHz and 7 GHz to 9 GHz.
The use of non active elements in the measurement configuration, in order to avoid non desired factors that could affect the collected data, made the calibration operation necessary. Following the VNAs manual recommendations, the calibration thru response type was selected , the cables and the connectors were included in this calibration. As we have the channel transfer function $H(f)$ in the frequency domain, to obtain an approximation of the channel impulse response (CIR) $h(t)$, we use the Inverse Fast Fourier Transform [9], as it is implemented in MATLAB6 library.

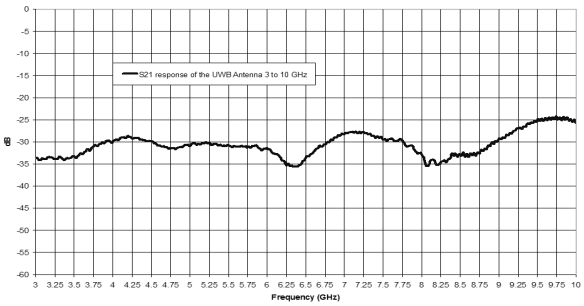

Fig. 1. S21 Response for the SkyCross UWB Antenna

B. Measurement Environment

Measurements are performed at spatially different locations for both Line-Of Sight (LOS) and Non Line Of Sight (NLOS). The experiment area is set by fixing the transmitting antenna on a mast at 1 m above the ground on horizontal linear grid (20 cm) close to VNA and moving the receiver antenna to different locations on horizontal linear grid (50 cm) in 1 cm steps. The height of receiver

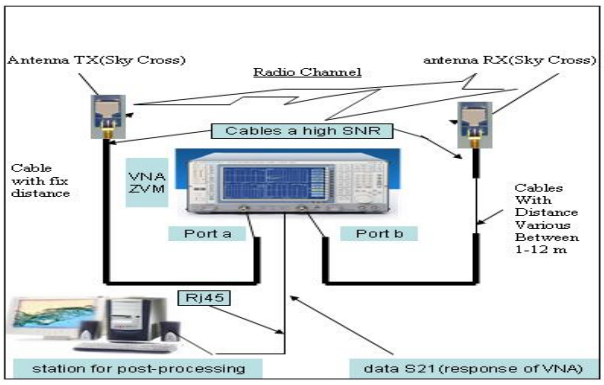

Fig. 2. Channel Measurement Setup

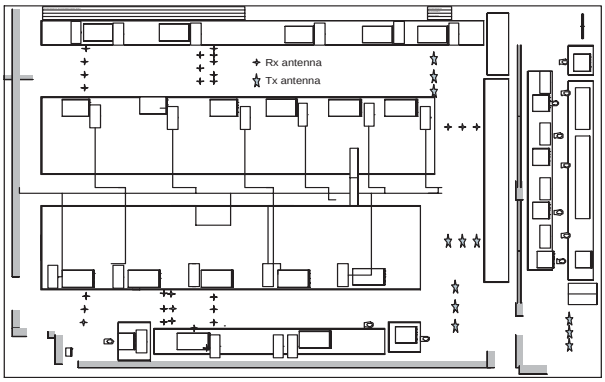

Fig. 4. Channel Measurement Environment

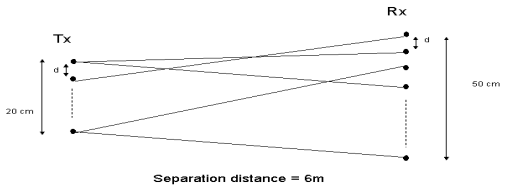

Fig. 3. Measurement configuration

antenna was also 1 m above the ground. The transmitter/receiver positioning is depicted in figure 3. This configuration targets peer-to-peer applications. For one scenario we sorted 3x50 different complex frequency responses. We repeat the same experiment for various separation between transmitter and receiving antennas varying from 1 meter to 12 meters. Among all positions, we considered both LOS and NLOS configurations. Measurements were carried out in Eurecoms Mobile Communication Laboratory, which has a typical laboratory environment (radio frequency equipment, computers, tables, chairs, metallic cupboard, glass windows,...) with plenty of reflective and diffractive objects, as shown in Figure 4, rich in reflective and diffractive objects. For the NLOS case, a metallic plate is positioned between the transmitter and the receiver. We have complete database of 4000 channel frequency responses corresponding to different scenarios with a transmitter-to-receiver distance varying distance varying from 1 meter to 12 metres.

III. UWB EIGENANALYSIS

A. Eigen-Decomposition Of Covariance Matrix

The radio-propagation channel is randomly time-varying due to variations in the environment and mobility of transmitters and receivers. It is classically represented, following the work of Bello [11], [12] by its input delay-spread function $h(t,\tau)$ called also, by abuse of language, the time-varying Channel Impulse Response (CIR). The variable t in the CIR notation represents the time-varying behavior of the channel caused by the mobility of either the transmitter, the receiver or the scatterers. The second variable τ represents the delay domain in which we characterize the channel regarding the most important arriving paths. We consider for each measurement a fixed position at the transmitter and the receiver sides, and a static environment (at least during the time-frame of one measurement). We are thus considering a static channel and we can then simplify the notation of the CIR by dropping its dependence on t. In what follows, $h(\tau)$ is simply replaced by $h(t)$. Let $\mathbf{h(t)} = [h_{W,1}(t), h_{W,2}(t), ..., h_{W,N}(t)]$ be the channel process obtained from measurements for N different antenna configurations, where $h_{W,i}(t)$ is expressed as

$$h_i(t) = g_i(t) + n_i(t), i = 1..N, \quad (1)$$

where $n_i(t)$ is zero-mean additive white Gaussian noise with power spectral density equal to σ_n^2 at all frequencies in the bandwidth of interest. We neglect any non-linear perturbation caused by measurement elements (e.g. VNA amplifiers), which were treated in a more general setting in [13]. We include the frequency response of the antenna as part of the channel response as argued in the previous section, and moreover, the linear response of the equipment is assumed to be perfectly accounted for in the calibration of the measurement apparatus. The noise process, resulting from thermal noise in the receive chain of the VNA and the noise generated by device itself, is assumed to be white in the band of interest. We therefore have that $\mathbf{g}(t) = [g_1(t), g_2(t), ..., g_N(t)]$ are the observations of the noise-free channel process corresponding to N observation positions. Due to the rapid variation of the wave's phase (from 0 to 2π over one wavelength), we can assume that the received electric field at each position represents a zero-mean process, and thus $g(t)$ is taken to be zero-mean. We remark that this does not rule out the possibility of line-of-sight propagation as will be treated shortly. The VNA provides samples of the observed channel process in the frequency domain, $H(k\Delta f)$, where Δf is the frequency separation, in our case 1 MHz. Furthermore, it is a filtered version of the channel response, where the filter corresponds to an ideal bandpass filter of bandwidth W centered at $f_c = (f_{\max} - f_{\min})/2$. After removing the carrier frequency f_c, we denote the complex baseband equivalent filtered channel by $h_W(t)$. By sampling the frequency response in the VNA we obtain an aliased version of $h_W(t)$ denoted by $\tilde{h}_W(t) = \sum_k h_W(t - k/\Delta f)$. The time-domain samples obtained by performing an inverse discrete Fourier transform (IDFT) on the vector $\mathbf{H} = \begin{pmatrix} H(0) & H(\Delta f) & \cdots & H((N-1)\Delta f) \end{pmatrix}^T$ are samples of $\tilde{h}_W(t)$ at sampling frequency W Hz. We note that the choice of frequency separation Δf has an impact on how closely $\tilde{h}_W(t)$ approximates $h_W(t)$ in the interval $[0, 1/\Delta f)$. In our case the choice of $\Delta f = 1$ MHz guarantees that the approximation will be very accurate since the typical delay spread of the considered channels is less than 100 ns and therefore time-domain aliasing will not distort

the channel measurement. For this reason we assume in what follows that the measurement equipment provides perfect samples of $h_W(t)$. Our approach to characterize the UWB propagation channel is based on the analysis of the channel subspace and the eigen-decomposition of the covariance matrix, $\mathbf{K_h}$, of the samples of $h_W(t)$, denoted by the vector $\mathbf{h} = \left(h_W(0) \quad h_W\left(\frac{1}{W}\right) \quad \cdots \quad h_W\left(\frac{p-1}{W}\right)\right)^T$, where p is the length of the channel used for statistical analysis with $0 \leq p \leq \frac{1}{\Delta F} - \frac{1}{W}$. This allows us to estimate the number of DoF characterizing $h_W(t)$ [14]. A similar approach for estimating the (finite) unknown number of Gaussian signals using a finite set of noisy observations is described in [15] [16]. These techniques amount to determining the finite dimension of the signal subspace. In order to estimate the true covariance matrix $\mathbf{K_h}$, we use statistical averages based on observations from (20×50) positions. The covariance matrix of measured channel samples, **h**, is written as

$$\mathbf{K}_\mathbf{g}^N = \mathbf{K}_\mathbf{h}^N = \frac{1}{N}\sum_{i=1}^{N} \mathbf{h}_i \mathbf{h}_i^H \tag{2}$$

The covariance matrix is Hermitian and positive definite. For this reason, a unitary matrix U exists such that the Karhunen-Loève (KL) expansion gives

$$K_h = U\Lambda U^H = \sum_{i=1}^{N} \lambda_i \psi_i \psi_i^H;\ U^H U = I_N, \tag{3}$$

where $\lambda_1 \geq \lambda_2 \geq ... \geq \lambda_N$, ψ_i is the i^{th} column of U and I_N is the $N \times N$ identity matrix with number of samples equal to N [18]. λ_i and ψ_i are the i^{th} eigenvalue and eigenvector of K_h, respectively. Decomposing (3) into principal and noise components yields

$$\begin{gathered} U_s = [\psi_1, \psi_2, ..., \psi_L]; \\ \lambda_1 \geq \lambda_2 \geq ... \geq \lambda_L; \\ U_n = [\psi_{L+1}, \psi_{L+2}, ..., \psi_N]; \\ \lambda_{L+1} \geq \lambda_{L+2} \geq ... \geq \lambda_N. \end{gathered}$$

where $U_s \perp U_n$. U_s defines the subspace containing both signal and noise components, whereas U_n defines the noise-only subspace. L is the number of significant eigenvalues which represents also the channel degrees of freedom.

Following the eigen-decomposition, and let $X = \|hh^*\|^2 / \overline{\|hh^*\|^2}$ we can express the channel-energy moment generating function as

$$G_X(s) = E\left[e^{sx}\right] = \int_{-\infty}^{+\infty} e^{sx} f_X(x) dx = L(f_X(x))|_{s=-s} \tag{4}$$

L is the Laplace transform operator and $f_X(x)$ is the probability density function (pdf) of variable X. We can see from last equation that $G_X(s)$ and $f_X(x)$ are Laplace transform pairs with $s = -s$. It is easily shown using the initial value theorem [17] that the probability density function of the normalized channel energy given by

$$f_X(x) = \sum_i \frac{\pi_i}{\mu_i} exp(-\frac{x}{\mu_i}) I(x.\mu_i > 0) \tag{5}$$

can be approximated around the origin for $0 \leq x << \min(\lambda_i(\mathbf{h}))$ as

$$f_X(x) \approx \frac{x^{(L-1)}}{(L-1)!} \frac{1}{\det(K_\mathbf{h})} = \frac{x^{(L-1)}}{(L-1)!} \frac{1}{\prod_i \lambda_i(\mathbf{h})} \tag{6}$$

his indicates that around the origin X behaves as an Erlang-L [1] variable with parameter $2\sigma^2 = \sqrt[L]{\prod_i \lambda_i(\mathbf{h})}$. The approximate cumulative distribution function (cdf) can be expressed in terms of the incomplete Gamma function, or in terms of the Marcum-Q function, $Q_L(0, x)$, as

$$F_X(x) = \frac{x^L}{\Gamma(L+1) \prod_i \lambda_i(\mathbf{h})} \tag{7}$$

From the expression of cdf we see that the slope of log(cdf) gives us an idea about the degrees of freedom of the channel or equivalently its inherent diversity. To avoid the imprecision caused by numerical IFFT, we decide to compute the eigenvalues λ_i directly from calculate the covariance matrix channel frequency response K_h obtained from the measurement campaign, by the use of Mtalab.

IV. Empirical UWB Channel Degrees Of Freedom Characterization Based On Eigenanalysis

A. Empirical Distribution Of Eigenvalues For UWB Channel

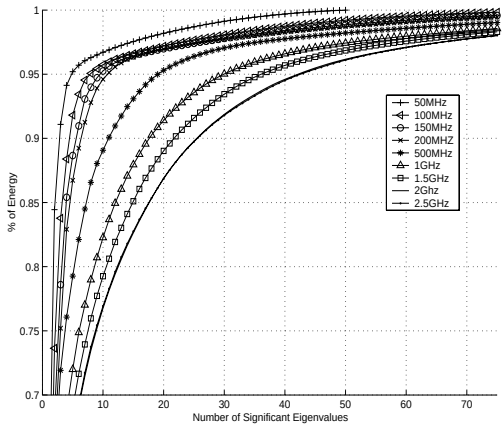

Fig. 5. Percentage of the captured energy versus number of significant eigenvalues in LOS situation, resolution 1 sample per megahertz

The empirical results presented in this paper are obtained from two scenarios with the following specifications: The transmitter-to-receiver distance is 6 meters, all antenna locations are in the laboratory and the configuration of measurement is shown in Figure 3. Each of three Tx positions corresponds to 50 Rx positions, leading to 3x50=150 complex frequency responses. The complex impulse response h(t) is calculated , but we limit the $h(t)$ to 1000 samples (1000 points) for the computation of Kh, from which Figures 10-14 are extracted.

In Figures 5 and 6 we plot, for LOS and NLOS settings, the percentage of the captured energy for M considered eigenvalues defined by $E_M = \frac{\sum_{i=1}^{M} \lambda_i}{\sum_{i=1}^{N} \lambda_i}$ with the total number of eigenvalues equal to N.

From both plots, we remark that for the narrow bandwidth case, the majority of whereas for the wide bandwidth case, the channel energy (more than 90%) is confined in small number of significant eigenvalues whereas in the wide bandwidth case, the channel energy is spread over a large number of eigenvalues (i.e. degrees of freedom). The results are obtained for the sampling rate in frequency domain, 1 sample per megahertz. This sampling resolution seems to be sufficient to capture all channel degrees of freedom. Figure 7 is plotted for 98% captured energy, and shows that the number of significant eigenvalues (i.e., the number of freedom degrees of the channel, as mentioned in part III), increases with the channel bandwidth. It is also noticed that starting from a certain bandwidth the number of significant

[1]The Erlang-L probability density function of variable X is given by $f_X(x) = \frac{x^{L-1}}{(2\sigma^2)^L \Gamma(L)} e^{-\frac{x}{2\sigma^2}}, x > 0$ and L aninteger

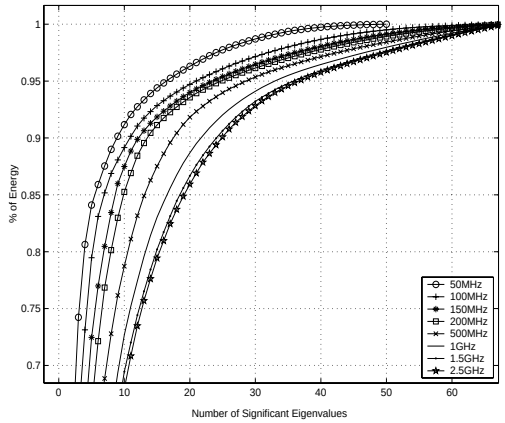

Fig. 6. percentage of the captured energy versus number of significant eigenvalues in NLOS situation,resolution 1 sample per megahertz

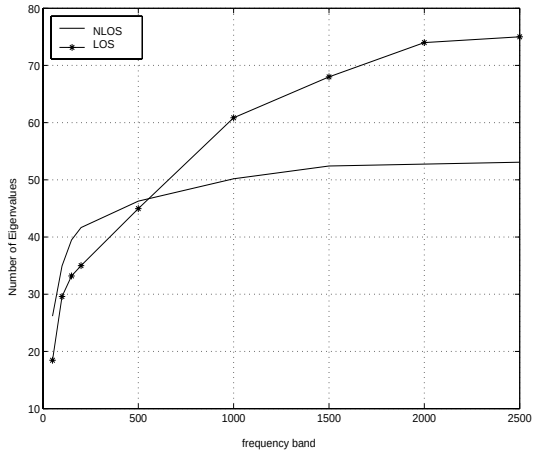

Fig. 7. Evolution number of eigenvalue for LOS and NLOS cases UWB measurement

eigenvalues increases slowly. This means that before this critical value the used signal bandwidth does not ensure a sufficient resolution to resolve all eigenvalues.

Figure 8 shows that the empirical cdf of the normalized energy for a 6 GHz bandwidth has a very sharp slope around the mean signal strength in comparison with a diversity 1 Rayleigh channel to highlight the extreme behavior of these channels. We also compare the empirical cdf curve to that one obtained using the integral of equation 5. We can pointed out that the number of significant eigenvalues is directley related to the sharpness of cdf curve. The high number of degrees of freedom shows that UWB channels can be considered as deterministic (non-fading) in practice, provided receivers exploiting the full channel energy are employed.

B. Eigenfunction Analysis In LOS And NLOS Situations

For the eigenfunctions or equivalently eigenvectors, gives an idea about the multi-paths dependency in propagation channel, also for explaining the relation between the eigenfunction and eigenvectors that the first is a presentation process in a continuous state and the second is a presentation process in a discrete state.

Figures 9, 10 and 11 show some sampled eigenfunctions in LOS settings corresponding to the most significant eigenvalues. These figures show that the channel exhibits a clustered behavior, as can be seen when we plot the power delay profile shown in Figures 12 and 13. It is remarkable that from our analysis we see that paths from different clusters have comparable strengths in the same eigenfunction which means a strongly dependent statistical behavior.

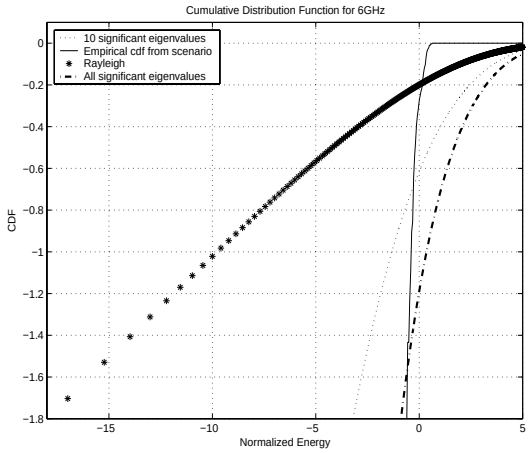

Fig. 8. The empirical Cumulative Distribution Function

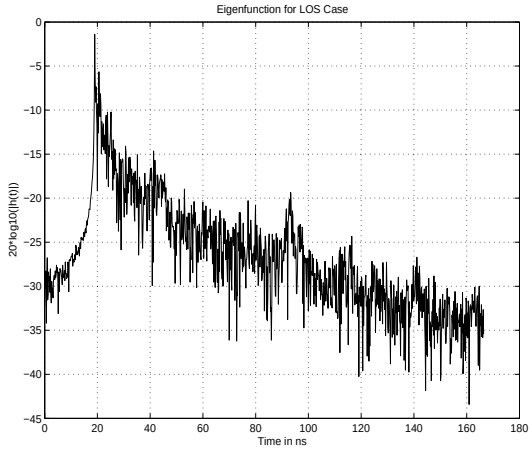

Fig. 9. Eigenfunction corresponding to $\lambda_1 = 0.4445$ in LOS situation

V. CONCLUSION

In this work we present results from UWB channel measurement campaigns conducted at Institut Eurécom laboratories. These measurements confirm previous results performed in other laboratories (e.g. [4]) regarding the clustered behavior of the UWB channel as well as the multipath richness exposed by the extreme bandwidth. The new results published in this work are twofold; first we show the evolution of the number of channel eigenvalues as a function of the system bandwidth for both LOS and NLOS scenarios, where we see that the number of eigenvalues tends to saturate for the extreme bandwidth of UWB systems. This seems to suggest that all significant multipath components can be resolved. Secondly we show that there is a strong statistical dependence between paths coming from different clusters, which is assumed not to be the case in most propagation models.

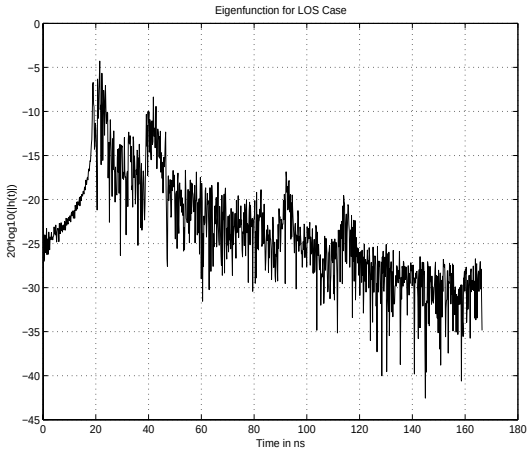

Fig. 10. Eigenfunction corresponding to $\lambda_5 = 0.0314$ in the LOS situation

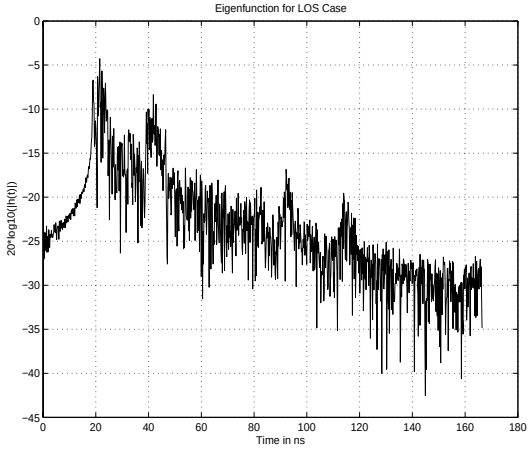

Fig. 11. Eigenfunction corresponding to $\lambda_{10} = 0.0133$ in LOS situation

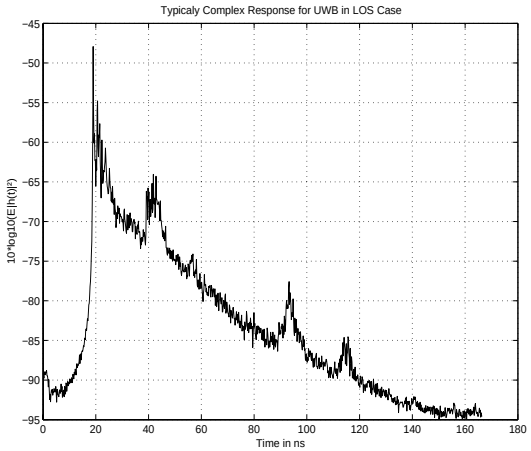

Fig. 12. Power Intensity Profile in LOS situation

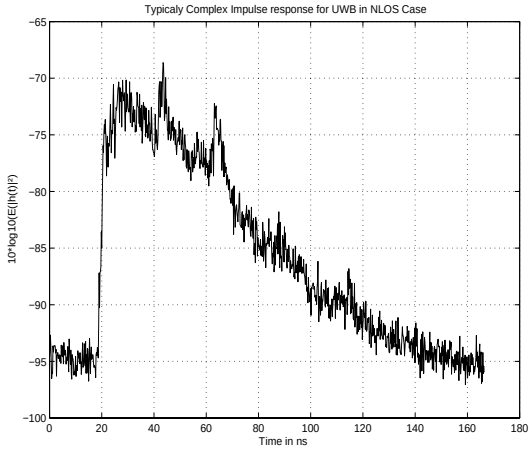

Fig. 13. Power Intensity Profile in NLOS situation

REFERENCES

[1] Scholtz, R. A. , "Multiple Access with Time-hopping Impulse Modulation", *MILCOM93, Belford, MA*, October 1993.

[2] Win, M. Z. , Scholtz, R. A. , "Impulse radio: how it works "*IEEE Communications Letters*, Volume: 2 Issue: 2, Pages: 36 -38, Feb. 1998.

[3] http://grouper.ieee.org.

[4] J. Kunisch and J. Pamp, "Measurement results and modeling aspects for UWB radio channel", UWBST 2002, Baltimore, May 2002.

[5] P. Pagani, P. Pajusco, S. Voinot, "A Study of the Ultra-Wide Band Indoor Channel: Propagation Experiment and Measurement Results", *IWUWBS Oulu, Finland*, June 2003.

[6] J. Foerster, "Channel Modeling Sub-comitee Report Final", IEEE P802.15 WG for WPANs Technical Report, no. 02/490r0-SG3a, 2002.

[7] Wilson R. D. , Weaver, R. D. , Chung, M. -H. , Scholtz, R. A. , "Ultra Wideband Interference Effects on an Amateur Radio Receiver", *IEEE Conference on Ultra Wideband Systems and Technologies*, 2002.

[8] www.skycross.com.

[9] John G. Proakis, Dimitris G. Manolakis "Digital Signal Processing: Principles, Algorithms and Applications" *Prentice-Hall, 3rd ed.*, 1996.

[10] Do-Sik Yoo, Victor W. -K. Cheng, Wayne E. Stark "An Index of Frequency Selectivity Frequency Mean Square Correlation ", *Proceedings of 51st VTC 2000-Spring, Tokyo, vol.3 pp. 2546-2550*

[11] Bello, Philip A., Characterization of Randomly Time-Variant Linear Channels, IEEE Transactions on Communications Systems, Vol. CS-11, pp. 360-393, 1963.

[12] Bello, Philip A., Time-Frequency Duality, IEEE Transactions on Information Theory, Vol. IT-10, pp. 18-33, 1964.

[13] G. Matz, A.F. Molisch, F. Hlawatsch, M. Steinbauer, I. Gaspard, "On the Systematic Measurement Errors of Correlative Mobile Radio Channel Sounders," IEEE Trans. on Communications, vol. 50, no. 5, May 2002

[14] D. Slepian and H.O. Pollak, "Prolate Spheroidal Wave Functions, Fourier Analysis, and Uncertainty- I,", Bell System Tech. J., vol. 40, pp. 43-64, 1961.

[15] M., Wax, T., Kailath, Detection of signals by information theoretic criteria, IEEE Transactions on , Volume: 33 , Issue: 2 , Apr 1985 Pages:387 - 392.

[16] D.B. Williams, "Counting the Degrees of Freedom When Using AIC and MDL to Detect Signals," IEEE Trans. on Signal Processing, vol. 42. no. 11, Nov. 1994.

[17] A.V. Oppenheim, A.S. Willsky, I.T. Young "Signals and Systems," Prentice-Hall, London 1983.

[18] S. Haykin."Adaptive Filter Theory", *Third Edition, Prentice-Hall*, Upper Saddle Rive, NJ, 1996.

[19] M. Schwartz, W. R. Bennet and S. Stein, "Communication Systems and Techniques", *New York: McGraw-Hill*, 1966